

Energy condition bounds and their confrontation with supernovae data

M. P. Lima,^{*} S. Vitenti,⁺ and M. J. Rebouças[‡]

Centro Brasileiro de Pesquisas Físicas, Rua Dr. Xavier Sigaud 150, 22290-180 Rio de Janeiro-RJ, Brazil
(Received 4 February 2008; revised manuscript received 6 March 2008; published 29 April 2008)

The energy conditions play an important role in the understanding of several properties of the Universe, including the current accelerating expansion phase and the possible existence of the so-called phantom fields. We show that the integrated bounds provided by the energy conditions on cosmological observables such as the distance modulus $\mu(z)$ and the lookback time $t_L(z)$ are not sufficient (or necessary) to ensure the local fulfillment of the energy conditions, making explicit the limitation of these bounds in the confrontation with observational data. We recast the energy conditions as bounds on the deceleration and normalized Hubble parameters, obtaining new bounds which are necessary and sufficient for the local fulfillment of the energy conditions. A statistical confrontation, with $1\sigma - 3\sigma$ confidence levels, between our bounds and supernovae data from the *gold* and *combined* samples is made for the recent past. Our analyses indicate, with 3σ confidence levels, the fulfillment of both the weak energy condition (**WEC**) and dominant energy condition (**DEC**) for $z \leq 1$ and $z \lesssim 0.8$, respectively. In addition, they suggest a possible recent violation of the null energy condition (**NEC**) with 3σ , i.e. a very recent phase of superacceleration. Our analyses also show the possibility of violation of the strong energy condition (**SEC**) with 3σ in the recent past ($z \leq 1$), but interestingly the $q(z)$ -best-fit curve crosses the **SEC**—fulfillment divider at $z \approx 0.67$, which is a value very close to the beginning of the epoch of cosmic acceleration predicted by the standard concordance flat Λ CDM scenario.

DOI: [10.1103/PhysRevD.77.083518](https://doi.org/10.1103/PhysRevD.77.083518)

PACS numbers: 98.80.Es, 98.80.-k, 98.80.Jk

I. INTRODUCTION

In classical general relativity, if one wishes to study spacetime properties that hold for a variety of matter sources, it is suitable to impose the so-called *energy conditions* that limit the arbitrariness of the energy-momentum tensor $T_{\mu\nu}$ on physical grounds. These conditions can be stated in a coordinate-invariant way in terms of $T_{\mu\nu}$ and vector fields of fixed character (timelike, null, and spacelike). However, within the framework of the standard Friedmann-Lemaître-Robertson-Walker (FLRW) model, we only need to consider the energy-momentum tensor of a perfect fluid with density ρ and pressure p , i.e.,

$$T_{\mu\nu} = (\rho + p)u_\mu u_\nu - pg_{\mu\nu}, \quad (1)$$

so that the energy conditions take one of the following forms [1–3]:

$$\begin{aligned} \text{NEC: } & \rho + p \geq 0, \\ \text{WEC: } & \rho \geq 0 \quad \text{and} \quad \rho + p \geq 0, \\ \text{SEC: } & \rho + 3p \geq 0 \quad \text{and} \quad \rho + p \geq 0, \\ \text{DEC: } & \rho \geq 0 \quad \text{and} \quad -\rho \leq p \leq \rho, \end{aligned} \quad (2)$$

where NEC, WEC, SEC, and DEC correspond, respectively, to the null, weak, strong, and dominant energy conditions. Clearly, the ordinary matter in the form of

baryons or relativistic particles like photons and neutrinos satisfies these energy conditions.

From the theoretical point of view, the energy conditions have been used in different contexts to derive powerful results in a variety of situations. For example, the Hawking-Penrose singularity theorems invoke the SEC [1], the positive mass theorem assumes the DEC [4], while the proof of second law of black hole thermodynamics requires NEC [3,5].

On macroscopic scales relevant for cosmology, another important viewpoint is the confrontation of the energy-condition predictions with the observational data. In this regard, since the pioneering works by Visser [6], it has been shown that the energy conditions provide model-independent bounds on the cosmological observables, and a number of studies involving such bounds have been recently discussed in the literature [7–14] (see also the related Ref. [15]). Santos *et al.* [7,8] have derived bounds on the distance modulus, $\mu(z)$, for any spatial curvature k , and made a confrontation of the bound predictions with recent type Ia supernovae (SNe Ia) data. In Refs. [9,10], the confrontation of the NEC and SEC bounds with a *combined* sample of 192 supernovae was carried out providing similar and complementary results. They have also shown that the violation of *integrated* bounds [such as those on $\mu(z)$] at a given redshift z ensures the breakdown of the corresponding energy condition, without specifying at what redshift the energy-condition violation took place. In Ref. [11], model-independent energy-conditions bounds on the lookback time, $t_L(z)$, was derived and a confrontation with age estimates of galaxies was made. Sen and

^{*}penna@cbpf.br

⁺vitenti@cbpf.br

[‡]reboucas@cbpf.br

Scherrer [12] derived upper limits on the matter density parameter Ω_m from the WEC in a flat ($k = 0$) universe. In the recent Ref. [16], Cattoën and Visser have reviewed and complemented some aspects of Refs. [6–8,11]. Energy-conditions constraints on modified gravity models, such as the so-called $f(R)$ -gravity, have also been investigated in Ref. [13] and more recently in Ref. [14].

In this paper, to proceed further with the investigation of the interrelation between energy conditions on scales relevant for cosmology and observational data, we extend and complement the results of Refs. [7–11] in three different ways. First, we show in a simple way that the violation of *integrated bounds* such as those on the Hubble parameter $H(z)$, on the distance modulus $\mu(z)$ [7,8], and on the lookback time $t_L(z)$ [11] at a redshift z is neither a necessary nor sufficient *local condition* for the breakdown of the associated energy condition [9,10]. Second, we derive *local necessary and sufficient* bounds for the fulfillment of each energy condition in terms of the deceleration parameter $q(z)$ and the normalized Hubble function $E(z) = H(z)/H_0$ for any spatial curvature. Third, we make the confrontation between our local *nonintegrated bounds* with statistical estimates [in the plane $E(z) - q(z)$] by using the SNe Ia of both the new *gold* sample [17], of 182 SNe Ia and the combined sample of 192 SNe Ia [18]. In this way, our necessary and sufficient nonintegrated energy-condition bounds allow a statistical confrontation of energy conditions and SNe Ia data within chosen confidence levels at any given redshift.

II. INTEGRATED BOUNDS FROM THE ENERGY CONDITIONS

In this section we give an account of our basic assumptions, briefly recast the major results of Refs. [7–10], and discuss the nature of the energy-condition integrated bounds and their limitation in the local confrontation with observational data.

Let us begin by recalling that the standard approach to cosmological modelling commences with a spacetime manifold endowed with the Friedmann-Lemaître-Robertson-Walker (FLRW) metric

$$ds^2 = dt^2 - a^2(t) \left[\frac{dr^2}{1 - kr^2} + r^2(d\theta^2 + \sin^2\theta d\phi^2) \right], \quad (3)$$

where the spatial curvature $k = 0, 1$, or -1 , and $a(t)$ is the cosmological scale factor. The metric (3) encodes the assumption that our 3-dimensional space is homogeneous and isotropic at sufficiently large scales along with the existence of a cosmic time t . However, to study the dynamics of the Universe an additional assumption in this approach to cosmological modeling is necessary, namely, that the large scale structure of the Universe is essentially governed by the gravitational interactions, and hence can be described by a metrical theory of gravitation such as general relativity (GR).

These very general premises, which we assume in this work, constrain the cosmological fluid to be a perfect-type fluid of the form (1), with the total density ρ and pressure p given by

$$\rho = \frac{3}{8\pi G} \left[\frac{\dot{a}^2}{a^2} + \frac{k}{a^2} \right], \quad (4)$$

$$p = -\frac{1}{8\pi G} \left[2\frac{\ddot{a}}{a} + \frac{\dot{a}^2}{a^2} + \frac{k}{a^2} \right], \quad (5)$$

where dots denote derivative with respect to the time t .

The integrated bounds on the Hubble functions $H(z)$ comes from the following set of dynamical constraints:¹

$$\mathbf{NEC} \Rightarrow -\frac{\ddot{a}}{a} + \frac{\dot{a}^2}{a^2} + \frac{k}{a^2} \geq 0, \quad (6)$$

$$\mathbf{WEC} \Rightarrow \frac{\dot{a}^2}{a^2} + \frac{k}{a^2} \geq 0, \quad (7)$$

$$\mathbf{SEC} \Rightarrow \frac{\ddot{a}}{a} \leq 0, \quad (8)$$

$$\mathbf{DEC} \Rightarrow \frac{\ddot{a}}{a} + 2 \left[\frac{\dot{a}^2}{a^2} + \frac{k}{a^2} \right] \geq 0, \quad (9)$$

which can be easily derived from the energy conditions [Eqs. (2)] along with the above Eqs. (4) and (5). In fact, Eqs. (6)–(9) can be written in terms of the Hubble function, $H(z) = \dot{a}(t)/a(t)$, and its derivatives with respect to the redshift, $z = (a_0/a) - 1$, as

$$\mathbf{NEC} \Rightarrow \frac{\partial H^2}{\partial z} \geq -\frac{2k(1+z)}{a_0^2}, \quad (10)$$

$$\mathbf{WEC} \Rightarrow -\frac{k(1+z)^2}{a_0^2 H^2} \leq 1, \quad (11)$$

$$\mathbf{SEC} \Rightarrow \frac{\partial \ln H^2}{\partial z} \geq \frac{2}{(1+z)}, \quad (12)$$

$$\mathbf{DEC} \Rightarrow \frac{\partial}{\partial z} \left(\frac{H^2}{(1+z)^6} \right) \leq \frac{4k}{a_0^2(1+z)^5}, \quad (13)$$

where here and in what follows the subscript 0 stands for present-day quantities. Now, integrating the inequations (10), (12), and (13) in the interval $(0, z)$, where we assume that they hold, one obtains the following integrated bounds

¹In line with the usage in Refs. [7,8,11], here and in what follows we use the boldface-type to denote the energy-condition restriction that is not contained in any of the previous set of energy-conditions inequations [see Eq. (2)]. In this way, **NEC**, **WEC**, **SEC**, and **DEC** refer, respectively, to the following NEC, WEC, SEC, and DEC inequations: $\rho + p \geq 0$, $\rho \geq 0$, $\rho + 3p \geq 0$, and $\rho - p \geq 0$.

on Hubble function from the energy conditions:

$$\mathbf{NEC} \Rightarrow H(z) \geq H_0 \sqrt{1 - \Omega_{k0} + \Omega_{k0}(1+z)^2}, \quad (14)$$

$$\mathbf{SEC} \Rightarrow H(z) \geq H_0(1+z), \quad (15)$$

$$\mathbf{DEC} \Rightarrow H(z) \leq H_0(1+z) \sqrt{(1 - \Omega_{k0})(1+z)^4 + \Omega_{k0}}. \quad (16)$$

We note that the in equation (11) does not contain the derivative of $H(z)$, but clearly for $z = 0$ the **WEC** restricts the present-day curvature parameter to $\Omega_{k0} \equiv -k/(a_0 H_0)^2 \leq 1$.

The integrated bounds provided by the energy conditions on the distance modulus $\mu(z)$ can now be easily obtained from the above bounds on the Hubble function as follows. First, we recall that the distance modulus for an object at redshift z is defined by

$$\mu(z) \equiv m(z) - M = 5 \log_{10} \left(\frac{d_L(z)}{1 \text{ Mpc}} \right) + 25, \quad (17)$$

where m and M are, respectively, the apparent and absolute magnitudes, and d_L is given by

$$d_L(z) = \frac{c}{H_0} \frac{(1+z)}{\sqrt{|\Omega_{k0}|}} S_k \left(\sqrt{|\Omega_{k0}|} \int_0^z \frac{dz'}{E(z')} \right), \quad (18)$$

where $S_k(x) = \sin(x)$, x , $\sinh(x)$ for $k = 1, 0, -1$ respectively, and $E(z) = H(z)/H_0$. Second, we substitute Eqs. (14)–(16) into Eqs. (17) and (18) to obtain the bounds on the distance modulus $\mu(z)$ for any spatial curvature k . For the flat FLRW model ($\Omega_{k0} = 0$) which we focus our attention on in this paper, the integrated bounds reduce to

$$\mathbf{NEC} \Rightarrow \mu(z) \leq 5 \log_{10} [cH_0^{-1} z(1+z)] + 25, \quad (19)$$

$$\mathbf{SEC} \Rightarrow \mu(z) \leq 5 \log_{10} [cH_0^{-1} (1+z) \ln(1+z)] + 25, \quad (20)$$

$$\mathbf{DEC} \Rightarrow \mu(z) \geq 5 \log_{10} \left[\frac{cH_0^{-1} z(2+z)}{2(1+z)} \right] + 25. \quad (21)$$

Concerning the above bounds on $H(z)$ and $\mu(z)$, we emphasize that the *nonlocal* or integrated nature of these bounds arises from the fact that they were obtained by assuming the fulfillment of the energy condition in the whole interval of integration $(0, z)$. However, in the same way that a positive sum of N terms does not necessarily imply that all the terms of the sum are also positive, the fulfillment of the integrated bounds on $H(z)$ and $\mu(z)$ does not necessarily imply that the energy conditions are obeyed in all subintervals of $(0, z)$ but only in at least an undetermined subinterval. Reciprocally, the violation of these

integrated bounds merely implies that the corresponding energy condition was violated in at least a subinterval of $(0, z)$. This amounts to saying that the fulfillment (or the violation) of any of these bounds at a given redshift z is not a sufficient (nor a necessary) local condition for the fulfillment (or, respectively, the violation) of the associated energy condition at z . In practice, this means that the local confrontation between the prediction of the integrated bounds such as those on $H(z)$ and on $\mu(z)$ [Eqs. (14)–(16)] and [Eqs. (19)–(21)] and observational data is not suitable to draw conclusions on the local fulfillment or violation of the associated energy conditions at z .²

III. NONINTEGRATED BOUNDS FROM THE ENERGY CONDITIONS

The practical limitation in the local confrontation between the above integrated bounds and observational data calls for nonintegrated bounds from energy conditions, which can be easily obtained by rewriting Eqs. (6)–(9) in terms of the deceleration parameter, $q(z) = -\ddot{a}/aH^2$, and the normalized Hubble function, $E(z) = H(z)/H_0$, in the following form:

$$\mathbf{NEC} \Leftrightarrow q(z) - \Omega_{k0} \frac{(1+z)^2}{E^2(z)} \geq -1, \quad (22)$$

$$\mathbf{WEC} \Leftrightarrow \frac{E^2(z)}{(1+z)^2} \geq \Omega_{k0}, \quad (23)$$

$$\mathbf{SEC} \Leftrightarrow q(z) \geq 0, \quad (24)$$

$$\mathbf{DEC} \Leftrightarrow q(z) + 2\Omega_{k0} \frac{(1+z)^2}{E^2(z)} \leq 2, \quad (25)$$

for any spatial curvature Ω_{k0} .

Some words of clarification are in order here concerning the above bounds. First, we note that, for a fixed value of Ω_{k0} , Eq. (23) provides the **WEC** lower bound on normalized Hubble function $E(z)$ for any z , whereas Eqs. (22) and (25) give, respectively, the **NEC** and **DEC** bounds on parameters of the $E(z) - q(z)$ plane for any fixed redshift z_* . Also, the **SEC** lower bound [Eq. (24)] clearly holds regardless of the value of the spatial curvature. Second, since the bounds have been derived without making any integration (nonintegrated bounds), they are clearly sufficient and necessary to ensure the *local* fulfillment of the

²We note that at a nonlocal level, the fulfillment (or the violation) of each of these integrated bounds at a given z is sufficient to ensure only the fulfillment (or, respectively, the violation) of the associated energy conditions somewhere in at least a subinterval of the integration interval $(0, z)$, as discussed in Refs. [9,10] and concretely illustrate in Sec. IV B.

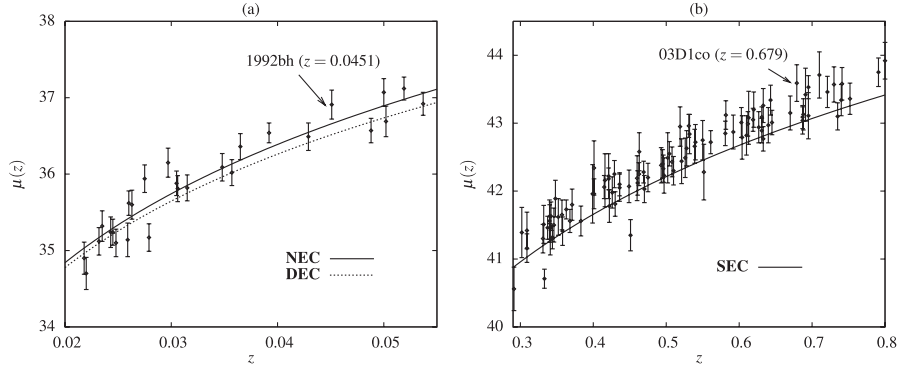


FIG. 1. (a) The **NEC** upper bound and the **DEC** lower bound on the distance modulus, $\mu(z)$, in the redshift interval (0.02, 0.055). (b) The **SEC** upper bound on $\mu(z)$ in the redshift interval (0.3, 0.8). The data points in both panels correspond to type Ia supernovae from a combined sample, and consistently we have taken $H_0 = 65.8 \text{ km s}^{-1} \text{ Mpc}^{-1}$.

associated energy condition. In practice, this allows local confrontation between the predictions of these *nonintegrated* bounds and, e.g., SNe Ia data, an issue which we shall discuss in the following sections focusing in the flat FLRW ($k = 0$) case, in which the **NEC** and **DEC** non-integrated bounds reduce, respectively, to $q(z) \geq -1$ and $q(z) \leq 2$, and where obviously the fulfillment of the **SEC** [$q(z) \geq 0$] implies that the **NEC** is satisfied identically.

IV. ANALYSIS AND DISCUSSION

A. Estimates of $q(z_*)$ and $E(z_*)$

In order to make the confrontation between the non-integrated bounds [Eqs. (22)–(25)] with observational data we need estimates of $q(z_*)$ and $E(z_*)$. Model-independent estimates of these parameters can be obtained by approximating the deceleration parameter as a function of the redshift in terms of a linear piecewise continuous function, known as linear spline,

$$q(z) = q_l + q'_l \Delta z_l, \quad z \in (z_l, z_{l+1}), \quad (26)$$

where the subscript l means that the quantity is taken at z_l , $\Delta z_l \equiv (z - z_l)$, and the prime means the derivative with respect to z . We use the definition of $q(z)$ in terms of $H(z)$ to obtain

$$E(z) = \exp \int_0^z \frac{1 + q(z)}{1 + z} dz, \quad (27)$$

and, consequently, the luminosity distance and the distance modulus using Eqs. (17) and (18). Then we fitted the parameters of the $q(z)$ curve using the type Ia supernovae (SNe Ia) redshift-distance modulus data from the gold sample [17] and a combined sample [18].

B. Results

In Figs. 1(a) and 1(b) we confront, the **NEC** along with **DEC**, and the **SEC** integrated bounds on $\mu(z)$ [Eqs. (19)–(21)] with SNe Ia of the combined sample as compiled in Ref. [18] for, respectively, the redshift inter-

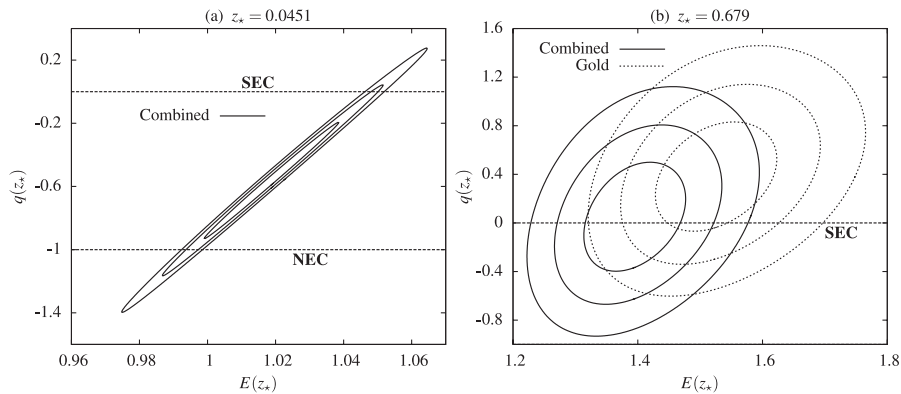


FIG. 2. The 1σ , 2σ , and 3σ contours obtained with the $E(z_*)$ and $q(z_*)$ estimates from combined (solid lines) and gold (dashed lines) samples at $z_* = 0.0451$ [panel (a)] and at $z_* = 0.679$ [panel (b)]. The nonintegrated **SEC** and **NEC** bounds are also indicated. The best-fit values for $(E(z), q(z))$ at $z_* = 0.0451$ are (1.015, -0.638) for gold, and (1.020, -0.559) for combined. At $z_* = 0.679$ the best-fit values are (1.621, 0.469) for gold, and (1.464, 0.215) for combined sample.

vals (0.02, 0.055) and (0.3, 0.8) by taking consistently $H_0 = 65.8 \text{ km s}^{-1} \text{ Mpc}^{-1}$.³

Clearly there are several SNe data points indicating the violation with more than 1σ of the integrated **NEC** and **SEC** upper bounds on $\mu(z)$, and two data points suggesting the violation of the *integrated* **DEC** lower bound on the distance modulus with $\geq 1\sigma$.

To concretely contrast the integrated and nonintegrated bounds by using supernovae observations, we consider, as a first example, the supernova 1992bh at $z = 0.0451$ of the combined sample, whose observed distance modulus is $\mu_{1992\text{bh}} = 36.91 \pm 0.19$ while the upper-bound **NEC** predictions is $\mu(z = 0.0451) = 36.66$, i.e., it violates the integrated upper bound from **NEC** with $\approx 1.31\sigma$ [see Fig. 1(a)]. However, this local violation of the **NEC** integrated bounds is not sufficient to guarantee the breakdown of the **NEC** at $z = 0.0451$. This point is made apparent in Fig. 2(a) which shows the 1σ , 2σ , and 3σ confidence regions in the plane $E(z) - q(z)$ [estimated from combined sample at $z_\star = 0.0451$] along with the nonintegrated (local) **NEC** bound [$q(z) \geq -1$]. Clearly, the fact that the whole 1σ confidence region is above the **NEC** nonintegrated bound is sufficient to ensure the fulfillment of the **NEC** with 1σ at $z_\star = 0.0451$, despite the $\approx 1.31\sigma$ violation of the **NEC** integrated bound at this redshift.

Figures 1(b) and 2(b) show the contrast between the **SEC** integrated and nonintegrated bounds. In Fig. 1(b) the supernova 03D1co (which belongs to the combined and gold samples) at $z_\star = 0.679$, is such that its observed value of the distance modulus [gold: $\mu = 43.58 \pm 0.19$, combined: $\mu = 43.59 \pm 0.27$] violated the **SEC** integrated upper-bound predictions [gold: $\mu = 43.06$, combined: $\mu = 42.99$] with 2.22σ (gold) and 2.72σ (combined). Figure 2(b) shows the 1σ , 2σ , and 3σ confidence regions in the plane $E(z) - q(z)$ [estimated from gold and combined sample at $z_\star = 0.679$] along with the nonintegrated **SEC** lower bound [$q(z) \geq 0$]. The comparison of these figures makes clear that although the observed $\mu(z)$ values are more than 2σ higher than the **SEC** integrated upper bounds (suggesting at first sight a violation of the **SEC**), the nonintegrated bound analysis shows that at $z_\star = 0.679$ the **SEC** can either be fulfilled or violated

³We note that for the combined sample provided by Riess [19], the distance modulus is computed using an arbitrary choice of the absolute magnitude M as discussed in [17,18]. In Fig. 1(a) and 1(b) we have dealt with this arbitrariness by noting that the confrontation between the integrated bounds [Eqs. (19)–(21)] with SNe Ia data depends on H_0 and M through the additive term $m_0 = M + 5\log_{10}\left(\frac{c}{H_0}\right)$. Thus, to obtain a value of m_0 consistent with the SNe data, we have fitted the low redshift ($z \leq 0.3$) SNe Ia distance modulus treating H_0 as an unknown and taking the values of magnitude M as given by the combined sample. Clearly, this procedure for comparison between bounds with SNe Ia data is independent of a particular value of H_0 in the sense that one can also begin by taking a specific value of H_0 , adjust the value of m_0 , and treating M as unknown instead.

within 1σ , 2σ , and 3σ confidence levels for both SNe Ia samples.

In order to obtain a detailed global picture of the breakdown and fulfillment of the energy conditions in the recent past, we shall extend the above local analysis by examining the behavior of the nonintegrated energy-condition bounds with $1\sigma - 3\sigma$ confidence levels for the recent past ($0 < z \leq 1$) using the combined and gold SNe Ia samples. To this end, we first divide the redshift interval (0,1] into 100 equally spaced points at which we carry out the statistical estimates and confrontation of the nonintegrated bounds with SNe Ia data. Second, we note that, for the flat case, the **NEC**, **SEC**, and **DEC** nonintegrated bounds do not depend on the estimates of $E(z_\star)$ [see Eqs. (22), (24), and (25) and Fig. 2], and therefore the upper and lower $1\sigma - 3\sigma$ limits of $q(z_\star)$ are sufficient to establish the fulfillment or violation of these energy conditions within these confidence levels.

The two panels in Fig. 3 show the best-fit values and 1σ , 2σ , and 3σ limits for $q(z_\star)$ for the combined [panel (a)] and gold [panel (b)] samples along with the nonintegrated **NEC**, **SEC**, and **DEC** bounds in the plane $q(z) - z$. These panels indicate the violation of the **SEC** with more than 3σ confidence level in the redshift intervals ($\approx 0.09, \approx 0.17$) and ($\approx 0.11, \approx 0.16$) for, respectively, the gold and combined samples. We note that highest evidence for the violation of **SEC** is at $z \sim 0.135$ for both samples [3.86σ (combined) and 3.43σ (gold) below the bound]. Clearly, violation of the **SEC** is also permitted (within 1σ to 3σ) for higher redshifts, but the best-fit $q(z_\star)$ curves cross the **SEC**-fulfillment divider at $z \approx 0.67$ and $z \approx 0.42$ for the combined and gold samples, respectively.

Concerning the **NEC**, the panels of Fig. 3 show its violation within 3σ for low redshifts [$z \in (0, \approx 0.1)$] for combined and gold samples. For higher values of redshift we have the **NEC**-fulfillment with 2σ for both samples.⁴ Regarding the **DEC**, Fig. 3 shows that it is fulfilled in nearly the whole redshift interval for both samples, but it might be violated within 3σ for high redshifts ($z \geq 0.8$), where the errors in our estimates grow significantly, though.

Concerning the above analyses it is worth emphasizing that they are very insensitive to the values of the curvature parameter, i.e., all the above conclusions remain essentially unchanged for values of Ω_{k0} lying in the interval

⁴Since the violation of the integrated bounds at any z ensures the violation of the associated energy condition in a subinterval $(0, z)$, the violation of the **NEC** within 1σ , in $z \in (0, 0.02)$ is the cause for the violation of the **NEC** integrated bound by the supernova 1992bh at $z = 0.0451$ of the combined sample. However, differently from the **NEC** case which is fulfilled with 1σ for $z > 0.05$, Fig. 3 shows no redshift where **SEC** is obeyed with 1σ . In this way, due to the degeneracies of the SNe Ia data, one cannot specify a subinterval of $(0, 0.679)$ responsible for the violation of the **SEC** integrated bound by SNe Ia 03D1co at $z = 0.679$.

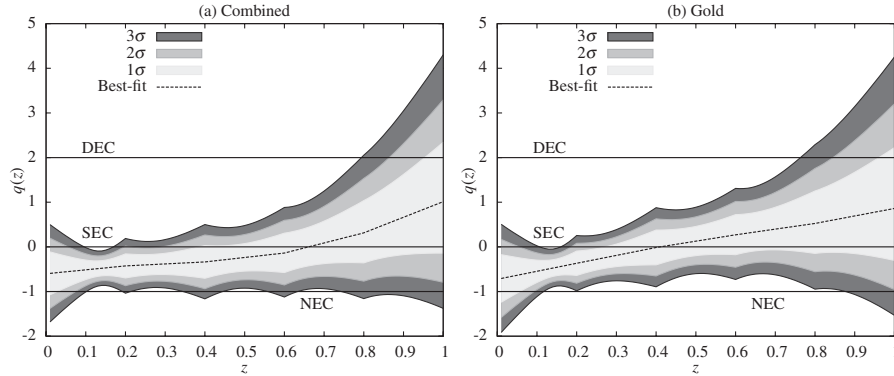


FIG. 3. The best-fit curve, the upper and lower 1σ , 2σ , and 3σ limits of $q(z)$ for 100 equally spaced redshifts. The **NEC** and **SEC** nonintegrated lower bounds, and also the **DEC** nonintegrated upper bound for the flat case are shown. This figure shows that the **SEC** is violated with 1σ confidence level until $z \approx 0.38$ for combined [panel (a)] and until $z \approx 0.26$ for gold sample [panel (b)]. It shows the violation of the **SEC** with 3σ for low redshift intervals. It also shows that the **NEC** and the **DEC** are violated within the 3σ confidence level for, respectively, very low and high redshifts. See the text for more details.

provided by the WMAP and other experiments [20]. In other words, our estimates of $E(z_*)$, $q(z_*)$ and of the nonintegrated bounds [Eqs. (22)–(25)] by using the best-fit value, the upper or the lower 1σ limits for $\Omega_{k0} = -0.014 \pm 0.017$ [20] are very close to estimates of those parameters in the flat case, with differences much smaller than the associated errors.

Finally, we also note that the nonintegrated **WEC** bound [Eq. (23)] is fulfilled in the whole redshift interval (0, 1) for the upper 1σ limit value of the curvature provided by WMAP team, i.e., $E^2(z) \geq 0.003(1+z)^2$ holds for all our estimated values of $E(z_*)$, whereas for the $\Omega_{k0} \in (-0.031, 0)$ the **WEC** is fulfilled identically, i.e., regardless of the values of $E(z_*)$ and z_* .

V. CONCLUDING REMARKS

By using the fact the classical energy conditions can be recast as a set of differential constraints involving the scale factor $a(t)$ and its derivatives [see (6)–(9)], model-independent integrated bounds on, e.g., the Hubble parameter $H(z)$, the distance modulus $\mu(z)$, and on the look-back time $t_L(z)$ have been recently derived and confronted with observational data (see, e.g., Refs. [6–11,16]).

In this paper, we have shown that the violation (or the fulfillment) of these integrated bounds at a given redshift z is neither sufficient nor necessary to ensure the violation (or, respectively, the fulfillment) of the energy conditions at z . In practice, this means that the local confrontation between the prediction of the integrated bounds and observational data (such as, e.g., those in Refs. [7,8,11]) is not sufficient to draw conclusions on the violation or fulfillment the energy conditions at z . This feature is also made apparent in Figs. 1 and 2, where we present concrete examples of violation of integrated bounds with either fulfillment of the nonintegrated bounds with 1σ [panels 1(a) and 2(a)], or fulfillment and violation

of the nonintegrated bounds with 1σ and 2σ [panels 1(b) and 2(b)].

To overcome the crucial drawback in the confrontation between integrated bounds on cosmological observables and observational data, we have formulated new bounds from energy conditions in terms of the normalized Hubble and deceleration parameters [$E(z)$ and $q(z)$] which are necessary and sufficient for the fulfillment of the energy conditions [Eqs. (22)–(25)]. We have also confronted our nonintegrated bounds with model-independent estimates of $q(z)$ and $E(z)$ which were obtained by using the gold sample of 182 SNe Ia provided by Riess *et al.* in Ref. [17] and with a combined sample of 192 SNe Ia provided by Wood-Vasey *et al.* [18] [Figs. 2 and 3]. On general grounds, our analyses indicate the **WEC** fulfillment in the recent past ($z \leq 1$) with 3σ , and a possible recent phase of superacceleration (violation of the **NEC** with 3σ for $z \in (0, 0.1)$) for both the combined and gold samples. Our analyses also show that the **DEC** is fulfilled with 3σ for all recent past redshifts but $z \geq 0.8$. Concerning the **SEC** our analyses indicate the possibility its violation with 1σ – 3σ confidence levels for $z \leq 1$, with small subintervals in which there is no **SEC**-fulfillment with 3σ for both the combined and gold samples. An interesting fact from the confrontation between the **SEC** nonintegrated bound and SNe Ia combined sample is that, although the violation of the **SEC** is permitted in the recent past with 3σ confidence level, the estimated $q(z)$ -best-fit curve crosses the **SEC**-fulfillment divider at $z \approx 0.67$ [see panel 3(a)], which is very close to redshift of the beginning of the epoch of cosmic acceleration predicted by the current standard concordance flat Λ CDM scenario with $\Omega_m \approx 0.3$.

Finally, we emphasized that, although we have focused our attention on the flat FLRW case, the above results concerning the new nonintegrated bounds analyses remain unchanged for values of Ω_{k0} lying in the interval provided by the WMAP team [20].

ACKNOWLEDGMENTS

This work is supported by Conselho Nacional de Desenvolvimento Científico e Tecnológico (CNPq)–Brasil, under Grant No. 472436/2007-4. M. P. L., S. V.,

and M. J. R. thank CNPq for the grants under which this work was carried out. M. J. R. also thanks J. Santos for valuable comments.

-
- [1] S. W. Hawking and G. F. R. Ellis, *The Large Scale Structure of Spacetime* (Cambridge University Press, England, 1973).
- [2] S. Carroll, *Spacetime and Geometry: An Introduction to General Relativity* (Addison-Wesley, New York, 2004).
- [3] R. M. Wald, *General Relativity* (University of Chicago Press, Chicago, 1984).
- [4] R. Schon and S. T. Yau, *Commun. Math. Phys.* **79**, 231 (1981).
- [5] M. Visser, *Lorentzian Wormholes* (AIP Press, New York, 1996).
- [6] M. Visser, *Science* **276**, 88 (1997); *Phys. Rev. D* **56**, 7578 (1997).
- [7] J. Santos, J. S. Alcaniz, and M. J. Rebouças, *Phys. Rev. D* **74**, 067301 (2006).
- [8] J. Santos, J. S. Alcaniz, N. Pires, and M. J. Rebouças, *Phys. Rev. D* **75**, 083523 (2007).
- [9] Y. Gong, A. Wang, Q. Wu, and Y. Z. Zhang, *J. Cosmol. Astropart. Phys.* **08** (2007) 018.
- [10] Y. Gong and A. Wang, *Phys. Lett. B* **652**, 63 (2007).
- [11] J. Santos, J. S. Alcaniz, M. J. Rebouças, and N. Pires, *Phys. Rev. D* **76**, 043519 (2007).
- [12] A. A. Sen and R. J. Scherrer, *Phys. Lett. B* **659**, 457 (2008).
- [13] S. E. Perez Bergliaffa, *Phys. Lett. B* **642**, 311 (2006).
- [14] J. Santos, J. S. Alcaniz, M. J. Rebouças, and F. C. Carvalho, *Phys. Rev. D* **76**, 083513 (2007).
- [15] C. Molina-París and M. Visser, *Phys. Lett. B* **455**, 90 (1999); D. Hochberg, C. Molina-París, and M. Visser, *Phys. Rev. D* **59**, 044011 (1999); S. M. Carroll, M. Hoffman, and M. Trodden, *Phys. Rev. D* **68**, 023509 (2003); P. Schuecker, R. R. Caldwell, H. Böhringer, C. A. Collins, L. Guzzo, and N. N. Weinberg, *Astron. Astrophys.* **402**, 53 (2003); J. Santos and J. S. Alcaniz, *Phys. Lett. B* **619**, 11 (2005); C. Cattoën and M. Visser, *J. Phys. Conf. Ser.* **68**, 012011 (2007); T. Qiu, Y.-F. Cai, and X.-M. Zhang, arXiv:0710.0115v1. See also the related articles: J. Zhou, B. Wang, Y. Gong, and E. Abdalla, *Phys. Lett. B* **652**, 86 (2007); M. Seikel and D. J. Schwarz, *J. Cosmol. Astropart. Phys.* **02** (2008) 007; V. K. Onemli and R. P. Woodard, *Classical Quantum Gravity* **19**, 4607 (2002); *Phys. Rev. D* **70**, 107301 (2004); M. Szydlowski and W. Czaja, *Phys. Rev. D* **69**, 083507 (2004); U. Alam, V. Sahni, T. D. Saini, and A. A. Starobinsky, *Mon. Not. R. Astron. Soc.* **354**, 275 (2004).
- [16] C. Cattoën and M. Visser, arXiv:0712.1619v1.
- [17] A. G. Riess *et al.* (High-*z* Supernova Search Team), *Astrophys. J.* **659**, 98 (2007); also arXiv:astro-ph/0611572v2.
- [18] W. M. Wood-Vasey *et al.*, *Astrophys. J.* **666**, 694 (2007); A. G. Riess *et al.*, *Astrophys. J.* **659**, 98 (2007); P. Astier *et al.* (SNLS Collaboration), *Astron. Astrophys.* **447**, 31 (2006); plus 45 nearby supernovae, see T. M. Davis *et al.*, *Astrophys. J.* **666**, 716 (2007), for details on this combined sample.
- [19] <http://braeburn.pha.jhu.edu/~ariess/R06/>
- [20] D. N. Spergel *et al.* (WMAP Collaboration), *Astrophys. J. Suppl. Ser.* **170**, 377 (2007).